Activity-Based Probes

Deutsche Ausgabe: DOI: 10.1002/ange.201607483
Internationale Ausgabe: DOI: 10.1002/anie.201607483

Isotopologous Organotellurium Probes Reveal Dynamic Hypoxia In Vivo with Cellular Resolution

*Landon J. Edgar, Ravi N. Vellanki, Trevor D. McKee, David Hedley, Bradly G. Wouters, and Mark Nitz**

Abstract: *Changes in the oxygenation state of microenvironments within solid tumors are associated with the development of aggressive cancer phenotypes. Factors that influence cellular hypoxia have been characterized; however, methods for measuring the dynamics of oxygenation at a cellular level in vivo have been elusive. We report a series of tellurium-containing isotopologous probes for cellular hypoxia compatible with mass cytometry (MC)—technology that allows for highly parametric interrogation of single cells based on atomic mass spectrometry. Sequential labeling with the isotopologous probes (SLIP) in pancreatic tumor xenograft models revealed changes in cellular oxygenation over time which correlated with the distance from vasculature, the proliferation of cell populations, and proximity to necrosis. SLIP allows for capture of spatial and temporal dynamics in vivo using enzyme activated probes.*

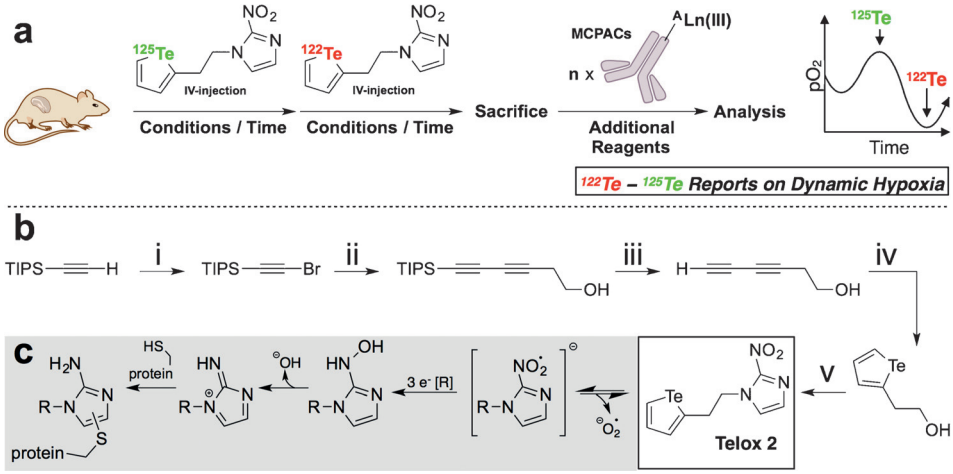

Figure 1. Design and synthesis of a probe for monitoring hypoxia dynamics. a) Schematic of the SLIP approach to measuring dynamic cellular hypoxia in vivo. Murine tumor models are injected with temporally spaced doses of isotopologues of Telox 2 followed by sacrifice, staining of cells with metal-chelating polymer–antibody conjugates and analysis of tumor tissue via MC. The difference in the quantity of tellurium isotopes reports on the oxygenation state of a cell at a given time point. In the plot on the right, a low ^{125}Te signal would be expected compared to ^{122}Te due to the lower pO_2 during exposure to ^{122}Telox 2. b) Reaction conditions: i) *N*-bromosuccinimide (1.15 equiv), $AgNO_3$ (1.0 equiv), acetone, RT, 3 hours, 85%. ii) 3-Butyn-1-ol (1.2 equiv), CuCl (2 mol%), 30% $BuNH_2$(aq.), 0°C→RT, 0.5 hours, 80%. iii) Tetrabutylammonium fluoride (TBAF) (4.0 equiv), THF, 0°C, 0.5 hours, not isolated. iv) Te^0, sodium hydroxymethylsulfinate (rongalite) (11.0 equiv), NaOH(aq.), 70°C, 4 hours, 90%. v) PPh_3 (1.05 equiv), DIAD (1.05 equiv), azomycin (1.05 equiv), THF, 0°C→RT, 3 hours, 90%. c) Mechanism of enzyme-mediated reduction of the 2-NI functionality to produce the electrophilic 2-nitrenium ion leading to non-specific protein labeling.[7c–e]

Regions with limited access to oxygen are common in solid tumors from many cancers.[1] Poor patient prognosis and an increased risk of metastasis have both been correlated with the degree of tumor hypoxia.[2] Cells exposed to repeated cycles of hypoxia and reoxygenation have a long-term survival advantage as compared with chronically hypoxic cells.[3] Cyclic hypoxia may be particularly important in its ability to activate pathways that promote metastasis, genomic instability, and resistance to treatment, but an understanding of temporal changes in hypoxia at the cellular level is largely lacking.[4] The ideal method for monitoring oxygenation dynamics would allow for highly parametric spatiotemporal analysis with cellular resolution. To achieve this, we turned to mass cytometry (MC); a technology that employs bioorthogonal heavy isotopes to report on a large (>40) number of biological parameters simultaneously.[5] MC is compatible with activity-based profiling of single cells using organotellurium mass tags, and we reasoned that this approach could be translated to spatiotemporal investigation of hypoxia using recently developed imaging MC (IMC).[6,7]

We envisioned an approach where isotopically coded tellurium-containing probes, which form covalent conjugates in hypoxic cells, could be serially injected into a tumor xenograft-bearing mouse. Changes in cellular hypoxia would

[*] Dr. L. J. Edgar, Prof. M. Nitz
Department of Chemistry, University of Toronto
80 St. George Street, Toronto, Ontario, M5S 3H6 (Canada)
E-mail: mnitz@chem.utoronto.ca
Dr. R. N. Vellanki, Dr. T. D. McKee, Dr. D. Hedley, Prof. B. G. Wouters
Departments of Radiation Oncology, Medical Biophysics, and the STTARR Innovaton Centre, Princess Margaret Cancer Centre, University Health Network
101 College Street, Toronto, Ontario, M5G 1L7 (Canada)

Supporting information for this article can be found under: http://dx.doi.org/10.1002/anie.201607483.

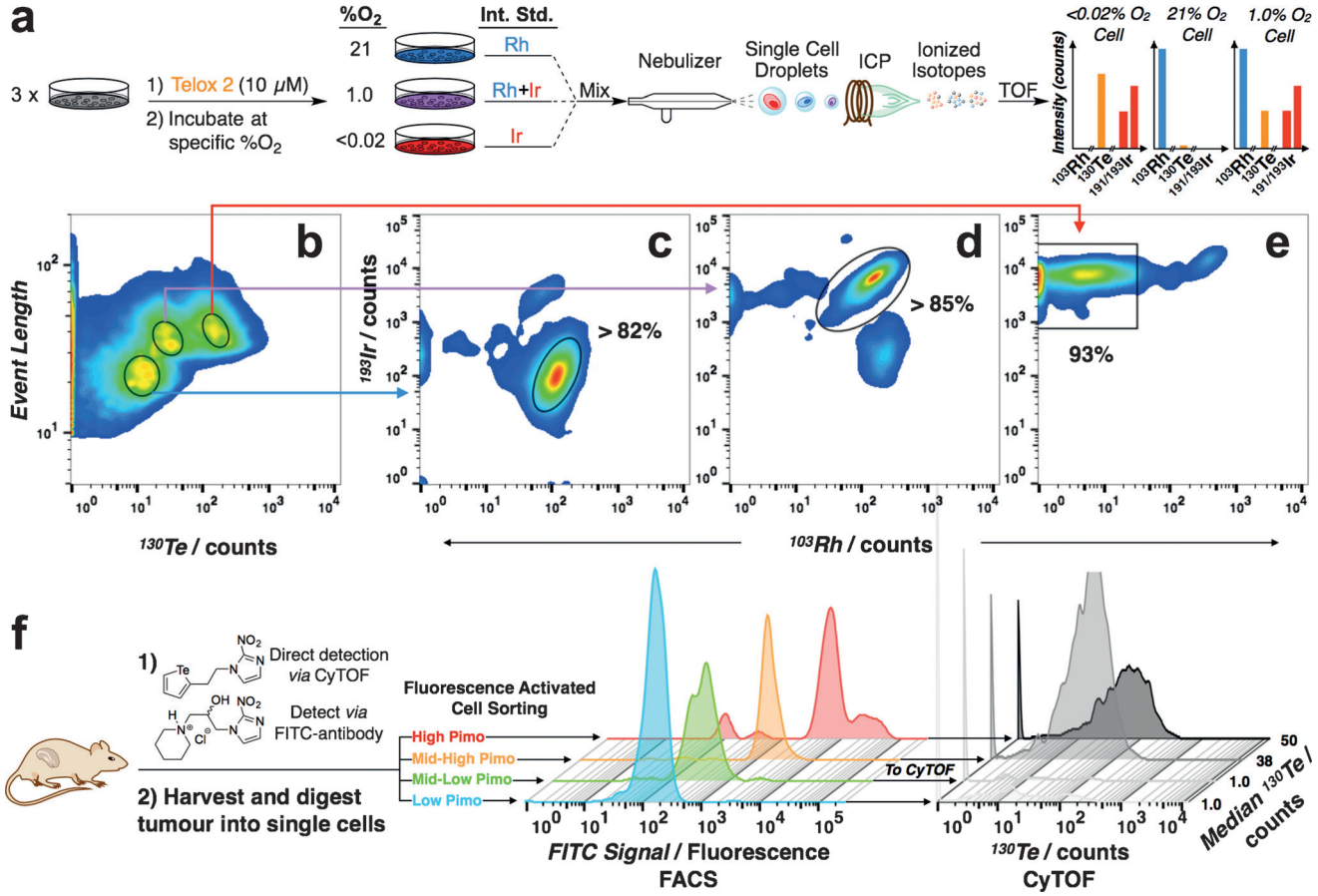

Figure 2. Evaluation of Telox 2 as a probe for cellular hypoxia in vitro and in vivo. a) PANC-1 cells in differently oxygenated atmospheres (3 h) were stained with metal-containing nucleic acid intercalators (^{103}Rh and/or $^{193/191}$Ir), mixed, and analyzed via MC. Cartoons of expected MC readouts are presented at right. b) Event length vs. ^{130}Te signal. c) Intercalator signals from low, d) intermediate, and e) high ^{130}Te gates. f) PANC-1 tumor xenograft-bearing SCID mice were co-injected with Telox 2 and Pimo (60 mg kg^{-1} each). After 3 h exposure, sacrifice, and digestion of tumor tissue, single cells were sorted via FACS and then analyzed by MC for ^{130}Te. Notes: All MC signals are reported as median values (arbitrary units). % of cells within drawn gates are indicated for (c)–(e).

be quantified by comparing tellurium isotope labeling by MC (Figure 1 a). This strategy of serial labeling with isotopologous probes (SLIP) has the unique advantage of removing complications that arise from using structurally different probes to report on the time-dependence of a biological phenomenon. Specifically, these isotopologous probes would have no significant differences in pharmacokinetics or metabolism that could confound interpretation of results, unlike other approaches to this type of strategy.[8]

Our previous MC-compatible hypoxia probe exhibited favorable activity in vitro, but failed to reliably identify hypoxic cells in vivo likely due to the stability of the telluroether.[7a] Chemical optimization of the organotellurium mass tag revealed that a more stable tellurophene would likely yield a better performing probe.[9] Indeed, combining a 2-nitroimidazole (2-NI) with a tellurophene produced a probe (Telox 2) with excellent solution stability and low toxicity both in vitro and in vivo (Figure 1 b; Supporting Information, Figures S1, S2, and S6). We reasoned that this probe would label hypoxic cells similarly to other 2-NI-bearing probes, where bioreductive metabolism converts the 2-NI to a 2-nitrenium imidazole which proceeds to non-specifically label nucleophile-bearing proteins (Figure 1 c).[7b–e]

The performance of Telox 2 was investigated in vitro using the human pancreatic cancer cell line PANC-1, which is known to form xenografts with a high hypoxic fraction.[10] Cells were incubated with Telox 2 under either near-anoxia (< 0.02 % O_2), hypoxia (1 % O_2), or normoxia (21 % O_2) (Figure 2 a). The cells were then washed, fixed, and coded by staining with one of three combinations of heavy isotope-containing nucleic acid intercalators (^{103}Rh and/or ^{193}Ir). The intercalator code allowed validation of the ^{130}Te signals from individual cells following mixing and analysis by MC (CyTOF2, Fluidigm). A density map of ^{130}Te vs. event length revealed three populations of cells (Figure 2 b). ^{103}Rh vs. ^{193}Ir output from each of these three populations retrieved the original nucleic acid staining combination expected for each population demonstrating that Telox 2 was capable of labeling cells in an oxygen concentration-dependent manner (Figure 2 c–e). Labeling with Telox 2 was found to be dose-dependent, linear with time, and was observed over a wide range of O_2 concentrations suggesting that Telox 2 may be used as a probe for measuring hypoxia on a gradient of O_2 (Supporting Information, Figures S3 and S4). Additionally,

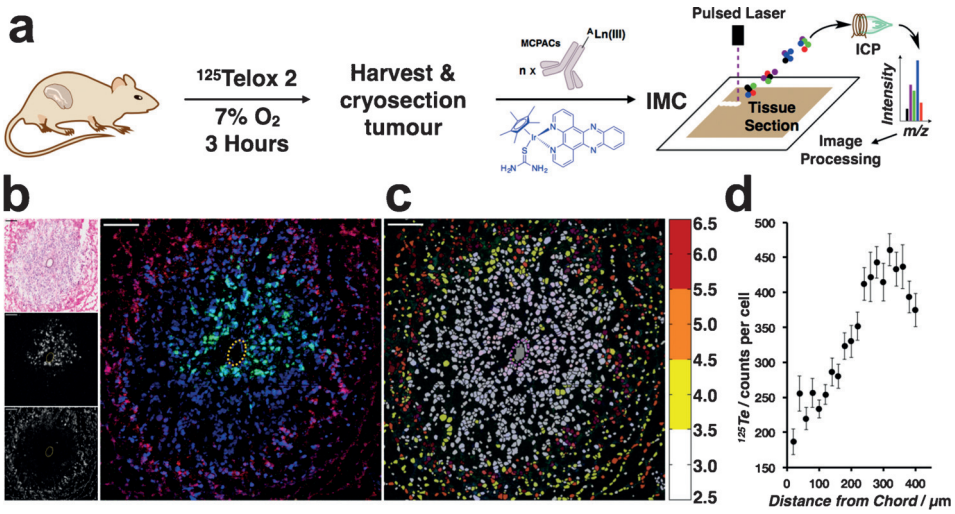

Figure 3. Isotopically enriched Telox 2 and imaging mass cytometry report on diffusion-limited hypoxia in vivo. a) A mouse bearing a PANC-1 tumor xenograft was injected with ^{125}Te-enriched Telox 2 (60 mg kg^{-1}). After 3 h the mouse was sacrificed, and the tumor cryosectioned. Tissue sections were stained with MC-compatible reagents (i.e. anti-Ki-67 antibody (^{168}Er-labeled) and $^{191/193}$Ir nucleic acid intercalator) and analyzed via IMC. b) Tissue from experiment in (a) stained with H&E (top). A separate adjacent section analyzed via IMC (large panel). Red = ^{125}Te (^{125}Telox 2), green = ^{168}Er (Ki-67), blue = ^{193}Ir (DNA intercalator). ^{168}Er (middle) and ^{125}Te (bottom) channels are in grayscale on left. c) Processed image of data from (b). Segmented cells are shaded on a thermal scale that represents the intensity of the ^{125}Te mass channel (thermal legend on the right, arbitrary units). d) ^{125}Te intensity as a function of distance from the blood vessel. The vertical axis represents the average ^{125}Te signal for each segmented cell within 20 µm-thick circular slices of increasing distance from the blood vessel. Error bars represent the standard deviation of ^{125}Te for all cells within the corresponding 20 µm thick circular slice. Note: Scale bars = 100 µm. The blood vessel is outlined with a dashed oval.

cellular Te accumulation was found to be potentiated by the over-expression of cytochrome P450 oxidoreductase (POR) in HCT116 cells, and reduced following POR knockout, consistent with the mechanism of action of the 2-NI activity-based group (Figure 1c; Supporting Information, Figure S5).[11]

Next, we confirmed the ability of Telox 2 to label hypoxic cells in vivo using the previously validated hypoxia probe pimonidazole (Pimo, Hypoxyprobe) as a reference (Figure 2f).[12] PANC-1 tumor xenograft-bearing mice were injected with both Pimo and Telox 2. After three hours the mice were sacrificed and the tumors excised/digested into single cells. These cells were then stained with a FITC-tagged antibody against Pimo conjugates and sorted using fluorescence-based flow cytometry (FACS) into four fractions. We reasoned that cells enriched in Pimo should also be enriched in Telox 2 since both probes were designed to label hypoxic cells using the same 2-NI-dependent mechanism. Injection of each fraction obtained through FACS into a CyTOF2 revealed Pimo-dependent enrichment of ^{130}Te, suggesting that the two probes labeled similar populations of cells in vivo.

We investigated parameters that would influence the ability of Telox 2 to measure dynamic changes in tumor hypoxia using the SLIP approach (Figure 1a). In order to obtain meaningful data from this type of experiment, it was necessary to understand when a second isotopologue of Telox 2 could be administered without interference from the first. Thus, we measured the circulating $t_{1/2}$ of the probe in murine plasma using LC/MS/MS.[13] This experiment indicated that a second isotopologue could be administered 12–16 hours (ca. $4\,t_{1/2}$) after the first, as the majority of the initial isotopologue would have cleared circulation by that time (Supporting Information, Figure S7). Additionally, we measured the in vitro stability of Telox 2 conjugates via MC to determine how long the tellurium mass tag would remain detectable in cells after reoxygenation (Supporting Information, Figure S8). Even after 48 hours tellurium levels were well above the limit of detection indicating that conjugates should remain detectable at the end of a SLIP experiment.

In order to evaluate dynamic cellular oxygenation in the context of underlying tissue morphology, we investigated Telox 2 labeling using IMC.[6] We synthesized isotopically enriched variants of Telox 2 containing either a ^{125}Te or ^{122}Te nucleus (>92% and >91% enrichment, respectively). Since ^{125}Te does not share a mass with any other stable isotope and ^{122}Te only shares its mass with a low-abundance (4.6%) isotope of tin, there should be no isotope background in the tissue.

Initially, a PANC-1 tumor xenograft-bearing mouse model was injected with ^{125}Telox 2 and introduced to an oxygen-reduced atmosphere (7% O_2) for 3 hours in order to promote an increase in tumor hypoxia (Figure 3a).[10] The tumor was then harvested, cryosectioned (5 µm), and stained with an antibody against the proliferation marker Ki-67 (labeled with ^{168}Er) and the $^{191/193}$Ir nucleic acid intercalator (an IMC-compatible surrogate for DAPI nuclear stain). IMC identified an example of diffusion-limited hypoxia, where the most intense ^{125}Te signal was detected in viable cells most distant from an apparent blood vessel, adjacent to necrosis, and anti-localized with proliferating cells as identified by H&E stain from an adjacent tissue section and the Ki-67 antigen, respectively (Figure 3b). Using a cell segmentation algorithm, the approximate size and shape of individual cells were traced and a ^{125}Te signal intensity assigned to each individual cell (Figure 3c). This data processing revealed that the maximum ^{125}Te signal was observed at a distance of ca. 300 µm (beyond the average diffusion distance of O_2 in tissue) from the blood vessel, and upon transition into necrotic tissue the signal decreased, likely due to decreased enzymatic activity in this region.[14]

We next investigated hypoxia dynamics using isotopologues of Telox 2. Mice with PANC-1 tumor xenografts were

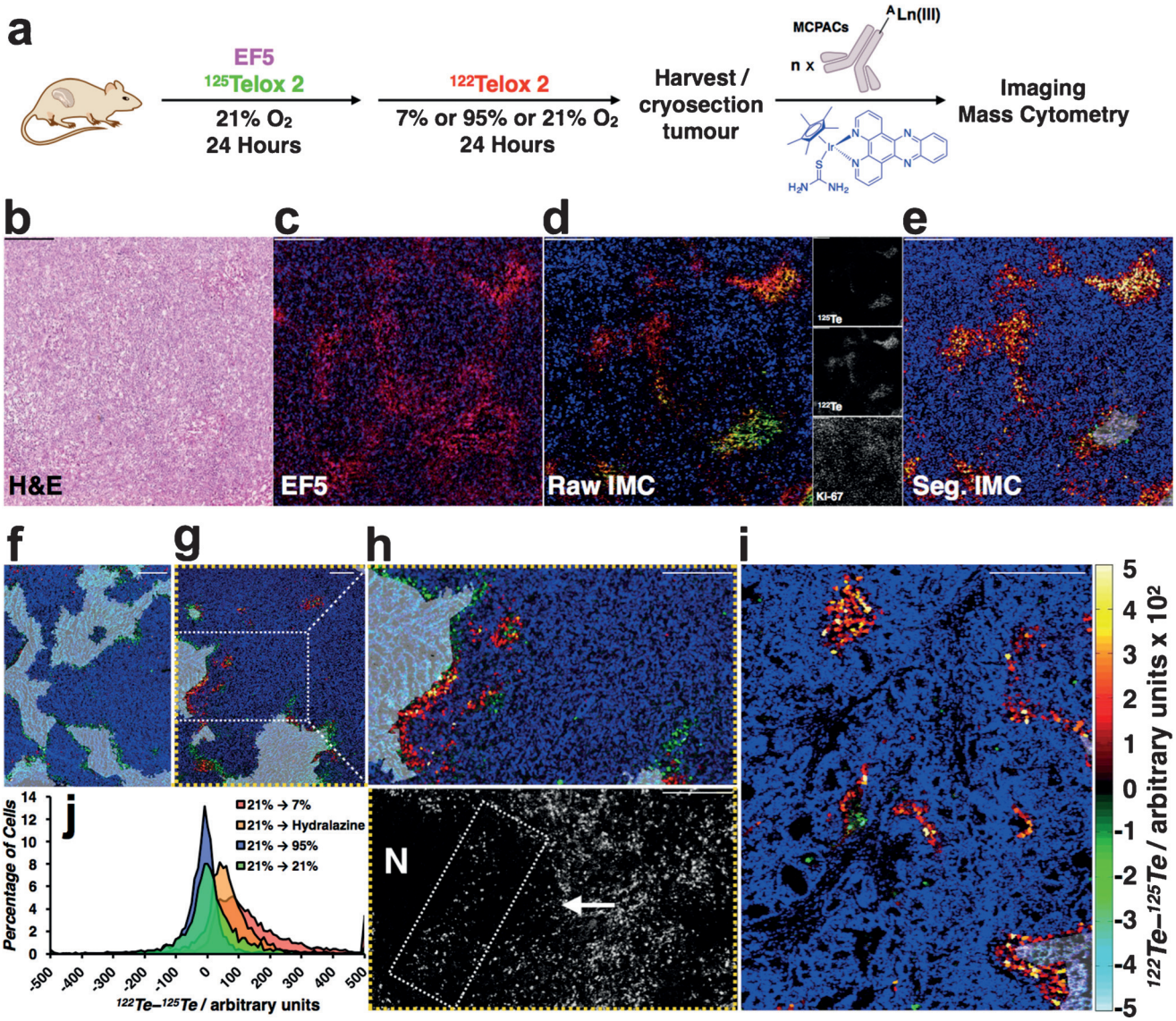

Figure 4. The SLIP strategy reports on dynamic hypoxia in pancreatic tumors. a) Schematic of a SLIP IMC experiment. Mice bearing PANC-1 tumor xenografts were injected with ^{125}Telox 2 + EF5 and left to breathe 21 % O_2. After 24 h, ^{122}Telox 2 was injected and animals were exposed to either 7 %, 95 %, or 21 % O_2. Sacrifice occurred 24 h later and tissues were processed as in Figure 3 a. b) H&E-stained section, c) fluorescence microscopy image (anti-EF5 antibody = pink, DAPI = blue), and d) raw IMC image of tissue from a reduced O_2-breathing (7 %) model. Red = ^{122}Te (^{122}Telox 2), green = ^{125}Te (^{125}Telox 2), blue = ^{168}Er (Ki-67). Individual mass channels on right. e) Processed image of data in (d). Segmented cells are shaded on a thermal scale (right of panel i) representing the value of ^{122}Te–^{125}Te. f) Processed image from an increased O_2-breathing (95 %) model, and g) constant normoxia (21 %) model. h) Enhanced view of (g). Ki-67 + (^{168}Er) cells are in the grayscale panel. Proposed region of hypoxic cell turnover and direction of cell displacement indicated by the white box and arrow, respectively. i) Processed image from a 21 % O_2-breathing OCIP-51 tumor model. j) Histograms of segmented cells from panels (e), (f), (g), and Figure S13. Notes: All probes dosed at 60 mg kg^{-1}. All scale bars = 400 μm. Blue channel in processed images is ^{193}Ir (nuclear stain). Gray masks mark necrotic zones.

injected with a mixture of ^{125}Telox 2 and EF5 (60 mg kg^{-1} each) and left to breathe normal atmosphere to establish baseline levels of hypoxia (Figure 4 a). After 24 hours the mice were injected with ^{122}Telox 2 and subsequently split into four treatment groups. The first group was transferred to a sealed chamber containing 7 % O_2, the second to a sealed chamber containing 95 % O_2, and the third was left in normal atmosphere (21 % O_2). The fourth group was injected with the vasodilator hydralazine one hour post-injection with ^{122}Telox 2 (Supporting Information, Figure S9). After an additional 24 hours the tumors were harvested and cryosectioned. Three adjacent tissue sections were stained for each tumor. The first was stained with H&E for brightfield imaging (Figure 4 b). The second was prepared for fluorescence microscopy via staining with Hoechst nuclear stain and a Cy5.5-labeled anti-EF5 antibody—a well-validated probe against hypoxia. The third adjacent tissue section was stained with reagents compatible with detection via IMC including the $^{191/193}$Ir-containing nucleic acid intercalator and the ^{168}Er-labeled anti-Ki-67 antibody. Fluorescence microscopy revealed regions of the tumor section that had been labeled with EF5. We used this information to guide our IMC experiments since this technology is currently lower-throughput than optical techniques making ablation of an entire

tumor section impractical (Figure 4c). As expected, a similar localization of EF5 (Cy5.5) and Telox 2 (^{125}Te) in adjacent sections was observed; co-localization was not expected as adjacent tissue sections were being examined and the structurally distinct probes have different pharmacokinetics (Figure 4c,d). Following IMC analysis, single cells were digitally segmented and the difference between signals for the two tellurium isotopes (^{122}Te–^{125}Te) was reported for each cell that exhibited significant labeling with either isotope (Figure 4e). We propose that cells exhibiting a value of ^{122}Te–^{125}Te >0 became increasingly hypoxic following administration of the second isotopologue whereas those with a value <0 became less hypoxic (reoxygenated). As expected, tumors from mice subjected to reduced O_2-breathing following injection of the second isotopologue exhibited a markedly increased number of cells with ^{122}Te–^{125}Te >0 as compared to mice subjected to increased O_2-breathing, where a high proportion of cells exhibited negative ^{122}Te–^{125}Te values (Figure 4e,f,j). Samples from the group treated with hydralazine after dosing with the second isotopologue also exhibited exacerbated hypoxia, consistent with reduction of blood flow through tumor vasculature as a result of lowered blood pressure (Figure 4j; Supporting Information, Figure S16).[15] In all cases, hypoxic regions were generally anti-correlated with cell proliferation as reported by the presence of Ki-67 (Figure 4d; Supporting Information, Figures S12, S21, S30, S39, and S48).

Having demonstrated that the SLIP approach could reveal controlled changes in oxygenation in vivo, we used these tools to measure hypoxia dynamics in a tumor model that was a closer analogue of a clinical situation. The fourth group of tumors, having not been subjected to artificial O_2 manipulation, were analyzed for regions of increased and decreased hypoxia taking place over 48 hours. Indeed, regions were detected that presented with either higher ^{125}Te, ^{122}Te, or near-equal quantities of both isotopes suggesting reoxygenation, reduced oxygenation, or no change during the second isotopologue-exposure phase, respectively (Figure 4g). Of particular interest was our observation of a region bordering necrosis that appeared to experience a dramatic increase in the number of hypoxic cells (Figure 4h). We speculate that proliferating cells displace cells close to the necrotic region, forcing them into an O_2-deficient microenvironment, thereby inducing hypoxia as reported by the ^{122}Telox 2 isotopologue. Our data suggests that without artificial O_2-manipulation nearly equal quantities of cells become newly hypoxic and newly normoxic over the time frame investigated (Figure 4j, green histogram). Dynamic changes in oxygenation were also observed in a patient-derived pancreatic cancer xenograft model demonstrating the general applicability of this approach to the study of different tumor types (Figure 4i).

Taken together, these data indicate that isotopologous probes compatible with IMC can provide a general approach for investigating dynamic biological phenomena with spatiotemporal resolution without confounding effects from differential pharmacology of distinguishable probes. Telox 2 shows promise for translation to the clinic to capture dynamic oxygenation as a biomarker for better understanding cancer biology and treatment.

Acknowledgements

The authors acknowledge Fluidigm for providing access to instrumentation, reagents, and expertise in collecting MC and IMC data. Specifically, we would like to thank D. Bandura, V. Baranov, T. Closson, O. Loboda, O. Ornatsky, and J. Watson. We also acknowledge Q. Chang for productive discussions and G. McKeown for assistance processing IMC data. Additionally, we recognize W. Wilson for providing access to the mutant HCT116 cell lines. The authors would like to acknowledge the Spatio-Temporal Targeting and Amplification of Radiation Response (STTARR) program and its affiliated funding agencies. Finally, the authors acknowledge funding from the Canadian Cancer Society, Natural Sciences and Engineering Research Council of Canada, and Fluidigm Canada.

Keywords: activity-based probes · cellular hypoxia · dynamic biology · mass spectrometry · tellurium

How to cite: *Angew. Chem. Int. Ed.* **2016**, *55*, 13159–13163
Angew. Chem. **2016**, *128*, 13353–13357

[1] W. R. Wilson, M. P. Hay, *Nat. Rev. Cancer* **2011**, *11*, 393–410.
[2] N. Rohwer, T. Cramer, *Drug Resist. Updates* **2011**, *14*, 191–201.
[3] P. Martinive, F. Defresne, C. Bouzin, J. Saliez, F. Lair, V. Grégoire, C. Michiels, C. Dessy, O. Feron, *Cancer Res.* **2006**, *66*, 11736–11744.
[4] M. W. Dewhirst, Y. Cao, B. Moeller, *Nat. Rev. Cancer* **2008**, *8*, 425–437.
[5] O. Ornatsky, D. Bandura, V. Baranov, M. Nitz, M. A. Winnik, S. Tanner, *J. Immunol. Methods* **2010**, *361*, 1–20.
[6] C. Giesen, H. A. O. Wang, D. Schapiro, N. Zivanovic, A. Jacobs, B. Hattendorf, P. J. Schüffler, D. Grolimund, J. M. Buhmann, S. Brandt, Z. Varga, P. J. Wild, D. Günther, B. Bodenmiller, *Nat. Methods* **2014**, *11*, 417–422.
[7] a) L. J. Edgar, R. N. Vellanki, A. Halupa, D. Hedley, B. G. Wouters, M. Nitz, *Angew. Chem. Int. Ed.* **2014**, *53*, 11473–11477; *Angew. Chem.* **2014**, *126*, 11657–11661; b) K. Tanabe, Z. Zhang, T. Ito, H. Hatta, S. Nishimoto, *Org. Biomol. Chem.* **2007**, *5*, 3745–3757; c) R. A. McClelland, R. Panicucci, A. M. Rauth, *J. Am. Chem. Soc.* **1985**, *107*, 1762–1763; d) J. L. Bolton, R. A. McClelland, *J. Am. Chem. Soc.* **1989**, *111*, 8172–8181; e) R. J. Hodgkiss, *Anti-Cancer Drug Des.* **1998**, *13*, 687–702.
[8] J. Russell, S. Carlin, S. A. Burke, B. Wen, K. M. Yang, C. C. Ling, *Int. J. Radiat. Oncol. Biol. Phys.* **2009**, *73(4)*, 1177–1186.
[9] H. Park, L. J. Edgar, M. A. Lumba, L. M. Willis, M. Nitz, *Org. Biomol. Chem.* **2015**, *13*, 7027–7033.
[10] N. Pham, J. M. M. M. Magalhaes, T. Do, J. Schwock, N. Dhani, P. Cao, R. P. Hill, D. W. Hedley, *Int. J. Cancer* **2009**, *124*, 280–286.
[11] J. Su, Y. Gu, F. B. Pruijn, J. B. Smaill, A. V. Patterson, C. P. Guise, W. R. Wilson, *J. Biol. Chem.* **2013**, *288*, 37138–37153.
[12] K. L. Bennewith, J. A. Raleigh, R. E. Durand, *Cancer Res.* **2002**, *62*, 6827–6830.
[13] C. J. Koch, *Methods Enzymol.* **2002**, *352*, 3–31.
[14] R. H. Thomlinson, L. H. Grey, *Br. J. Cancer* **1955**, *9*, 539–549.
[15] M. R. Horsman, M. Nordsmark, M. Hoyer, J. Overgaard, *Br. J. Cancer* **1995**, *72*, 1474–1478.

Received: August 2, 2016
Published online: September 22, 2016

